Second-harmonic generation from thick thermal oxides on Si(111): the influence of multiple reflections

C. W. van Hasselt, M. A. C. Devillers, and Th. Rasing

Research Institute for Materials, University of Nijmegen, Toernooiveld, NL 6525-ED Nijmegen, The Netherlands

O. A. Aktsipetrov

Physics Department, Moscow State University, Moscow, 119899, Russia

Received May 6, 1994; revised manuscript received August 29, 1994

Recently a number of second-harmonic-generation (SHG) experiments on (thick) oxide films on Si were performed as studies of the possible presence of strain, crystalline SiO_2, a static electric field, and roughness at the Si–SiO_2 interface. Large enhancements of the SHG anisotropy have been observed for thick oxide films. We show here that the SHG for thick thermal oxide films on Si(111) as a function of oxide thickness and angle of incidence is dominated by linear optics, owing to multiple reflections in the oxide film.

1. INTRODUCTION

Optical second-harmonic generation (SHG) and sum-frequency generation have become much used, versatile, and sensitive surface and interface probes.[1,2] The techniques derive their surface sensitivity from the symmetry breaking at an interface and are especially sensitive to surface symmetry and electronic structure. They may therefore be extremely useful for studying the technologically important Si–SiO_2 interfaces. Recently a number of such studies were performed, indicating the sensitivity of SHG to surface symmetry[3–5] and steps on vicinal surfaces.[6–8] The effects of strain,[9,10] interface charges and electric fields,[11] preparation and roughness,[12] the possible presence of a crystalline oxide interface layer,[13,14] and the oxide thickness[10,15] have been discussed. Given the importance of the Si–SiO_2 interface, these various observations and interpretations call for a more systematic approach to the applicability of SHG as a diagnostic interface probe. We have performed SHG measurements on thermal oxide films on Si(111), with film thicknesses ranging from 2 to 300 nm. We find that the changes in the *s*-polarized SHG signal as a function of oxide thickness and angle of incidence can be completely described by multiple reflections in the SiO_2 layer. The *p*-polarized results do suggest that there may be other SHG sources apart from the multiple-reflection effects.

2. THEORY

For a (111) surface of a cubic crystal, excited by a single *s*-polarized pump field at frequency ω, the *s*-polarized second-harmonic (SH) field $E_{s,s}$ can be written as[3,16,17]

$$E_{s,s}(2\omega) = b(\chi_{\xi\xi\xi} - a\zeta)\sin(3\psi), \tag{1}$$

where $\hat{\xi}$ is parallel to the $(11\bar{2})$ direction, $\chi_{\xi\xi\xi}$ is the anistropic surface contribution to $\overleftrightarrow{\chi}^{(2)}$, ζ is the bulk anisotropic contribution, ψ is the angle between $\hat{\xi}$ and the plane of incidence, and a and b are complex numbers containing the Fresnel factors for reflection. As can be seen from Eq. (1), bulk and surface contributions appear in the same way and therefore cannot be distinguished in a single measurement. Although in principle the Fresnel factors for surface and bulk are different, it has been shown that this difference is too small for the factors to be separated by scanning of the angle of incidence[17,18] owing to the high index of refraction of Si. For a stepped surface an estimation of the relative surface and bulk contribution can be made because of symmetry breaking by the steps.[6–8] For a flat Si(111) surface $E_{s,s}$ can be effectively characterized by one response parameter χ, and the reflected SH intensity $I_{s,s}$ can be written as

$$I_{s,s}(2\omega) \sim L_{2\omega}|\chi|^2 L_\omega{}^2 I^2(\omega)\sin(3\psi). \tag{2}$$

Here $I(\omega)$ is the pump intensity and L_ω and $L_{2\omega}$ are the linear Fresnel factors at ω and 2ω, respectively. The wave vectors for the fundamental and the SH field are matched by the nonlinear boundary condition[19]:

$$k_\parallel(2\omega) = 2k_\parallel(\omega). \tag{3}$$

For Si(111)–SiO_2 this model is consistent with SHG contributions from the silicon bulk, the Si–SiO_2 interface, and a possible SiO_x or crystalline SiO_2 transition layer. We exclude contributions from the SiO_2 bulk, as is expected for a centrosymmetric medium with low nonlinear response, and contributions from the SiO_2–air interface.

For an oxide film on a silicon substrate no extra contributions to SHG are expected, in contrast to some recent observations that report a distinct effect of the oxide thickness on SHG.[10,15] It can easily be shown, as is done in this paper, that these observations are mostly due to interference effects in the oxide layer that have to be taken into account before any other possible nonlinear sources are discussed.

Having a refractive index between that of air and silicon and negligible absorption for wavelengths from the UV to the IR, an oxide film on silicon can act as a resonator that can enhance the coupling of the fields into and

0740-3224/95/010033-04$06.00

out of the silicon. With such films described with a perfect three-layer model (air–SiO_2–Si), it is straightforward to write the Fresnel factors L_ω and $L_{2\omega}$.[20] For an incoming field in air at frequency ω and a certain oxide thickness the field at the Si–SiO_2 interface just inside the silicon is calculated and matched to the field at 2ω by use of Eq. (3). For this SHG field at the interface the transmission to the air is then calculated. Thus for a given χ of the Si–SiO_2 interface and Si bulk the dependence of $I_{s,s}$ on the angle of incidence and oxide thickness is completely described. Of course such a model can be extended to include more interfaces that do have an SHG response.[21,22]

3. EXPERIMENT

Our samples were p-type (2–5 Ω cm) Si(111) (±0.5°) wafers on which a 310-nm thermal oxide was grown at 1000° in a dry oxygen ambient environment. The wafers were annealed at a slightly higher temperature in a N_2 atmosphere to produce a smooth Si–SiO_2 interface. One wafer of the same batch with a native oxide of 2 nm was kept as a reference sample. Single-wavelength ellipsometry with a red He–Ne laser showed that the thickness of all samples was the same within 3 nm and that thickness variations on a single wafer were negligible. The refractive indices used in the ellipsometry were consistent with the ones used in the model for the SHG response. Before any modification SHG measurements on all samples were performed, showing the usual azimuthal anisotropies.[3–6] The size of the SHG signal was the same within 5% for all wafers but substantially larger than that from the reference sample. With a buffered NH_4F etching solution with an etching speed for SiO_2 of ~25 nm/min, some of the samples were etched in a 3 × 3 checkerboard configuration to produce stepped-oxide samples with nine different oxide thicknesses on one wafer. Thus we change the oxide thickness and the air–SiO_2 interface but leave the buried Si–SiO_2 interface the same. Before and after each etching treatment, ellipsometry was used to check the oxide thicknesses and to ensure good optical quality of the films over the whole sample.

For the SHG experiment the frequency-doubled output at 532 nm of a Q-switched Nd:YAG laser was used. The fluence of the 8-ns pulses was limited to 10 mJ in a 4-mm-diameter spot, well below the damage threshold and stable within 2%. The SHG signal was recorded with appropriate filters, a monochromator, a photomultiplier, and a gated integrator. Four samples were studied. One wafer was etched as a whole, and the s-polarized (p-polarized) SHG anisotropy for an s-polarized (p-polarized) pump beam $I_{s,s}$ ($I_{p,p}$) was measured for angles of incidence between 4° and 75° and two different oxide thicknesses (310 and 260 nm). These measurements were calibrated against the reference sample. The other three samples were prepared as stepped oxides, together ranging in oxide thickness from 2 to 310 nm, with some overlap between the different samples. On these $I_{s,s}$ was measured as a function of oxide thickness, at an angle of incidence of 4°, always showing a pure anisotropy. We measured the amplitude of this anisotropy on all oxide thicknesses by translating the sample through the laser beam, taking care to keep the alignment the same and to avoid measuring at the transition regions between different thicknesses. On one of these samples the linear reflection was measured with a green He–Ne laser at 544 nm for the same angle and polarizations.

4. RESULTS AND DISCUSSION

Figure 1 shows the amplitude of $I_{s,s}$ as a function of angle of incidence for oxide thicknesses of 310 (circles) and 260 nm (triangles) and for the reference sample with a native oxide (squares). All data are plotted on the same scale. The reference sample shows the characteristic monotonic decay from a maximum at 0° to zero at 90°.[8,16,17] Of course, multiple reflections play a minor role for this thin oxide. With, for Si, $n(\omega) = 4.151 + i0.052$ and $n(2\omega) = 1.854 + i4.438$,[23] the measurement is well described by our multiple-reflection model (solid curves). The measurements on the thick oxides show a large increase in SHG. Although the overall angle dependence is similar to that for the native oxide, now maxima appear at 25° (310 nm) and 55° (260 nm). For both thicknesses the azimuthal dependence contained only an anisotropic term, so no contribution from the oxide is included, which would be isotropic. Taking for SiO_2 $n(\omega) = 1.461$ and $n(2\omega) = 1.500$,[24] and using the same scaling parameter for both curves, we see that the measurements are well described by the multiple-reflection model both in amplitude and angle dependence. The dotted curve is the prediction from this model for a 2-nm oxide, given the amplitudes for 310 and 260 nm. It shows that the χ parameter of the thermal oxide is a factor of 1.2 larger than that of the native oxide. This difference indicates that these are two different interfaces and shows that SHG could be used to study the microscopic differences

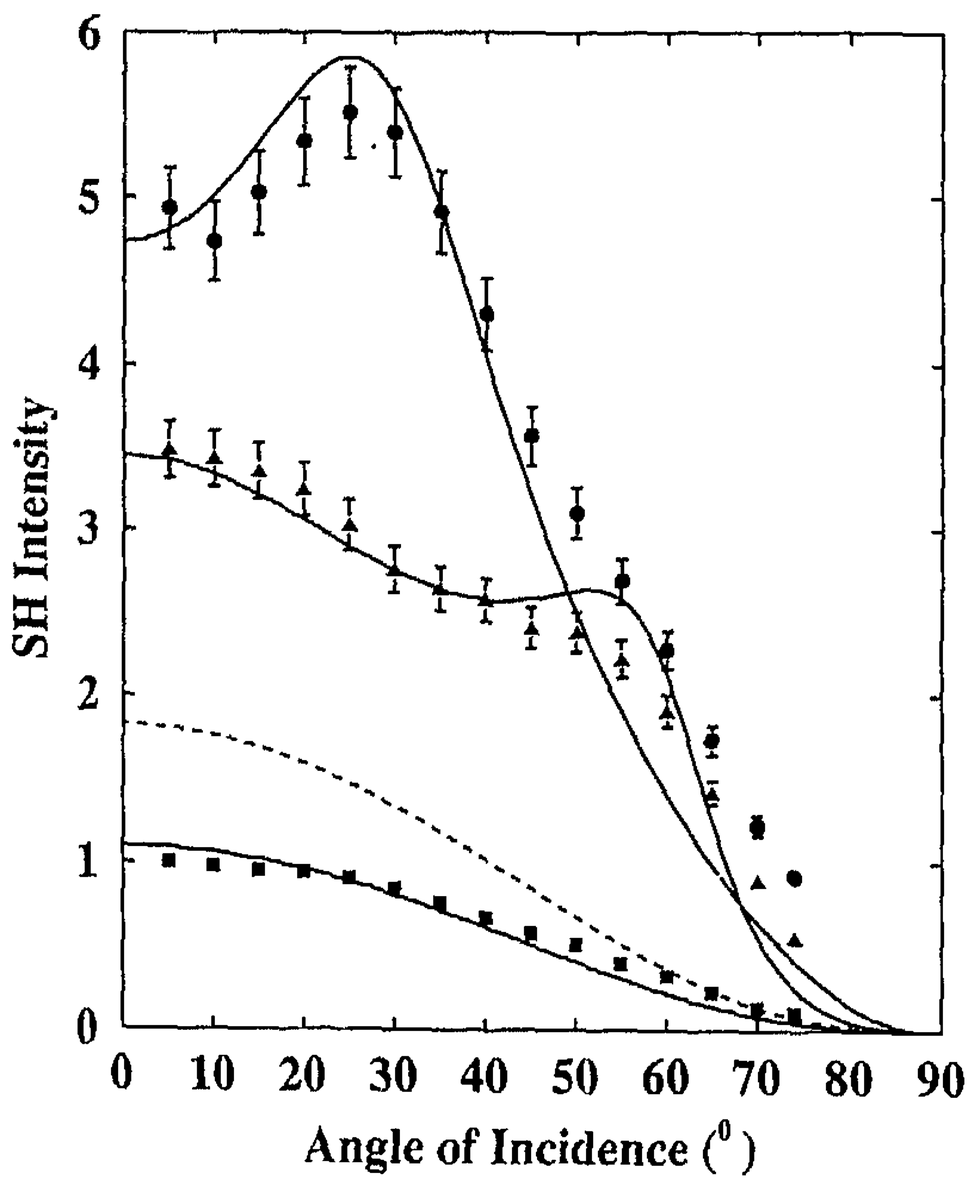

Fig. 1. Amplitude of $I_{s,s}$ as a function of angle of incidence for oxide thicknesses of 310 (circles), 260 (triangles), and 2 nm (squares). All measurements have been calibrated to the measurement on the 2-nm native oxide at 4°. The solid curves represent the model, where the scaling parameter is the same for 310- and 260-nm oxide, and the dotted curve is the prediction for a 2-nm thermal oxide.

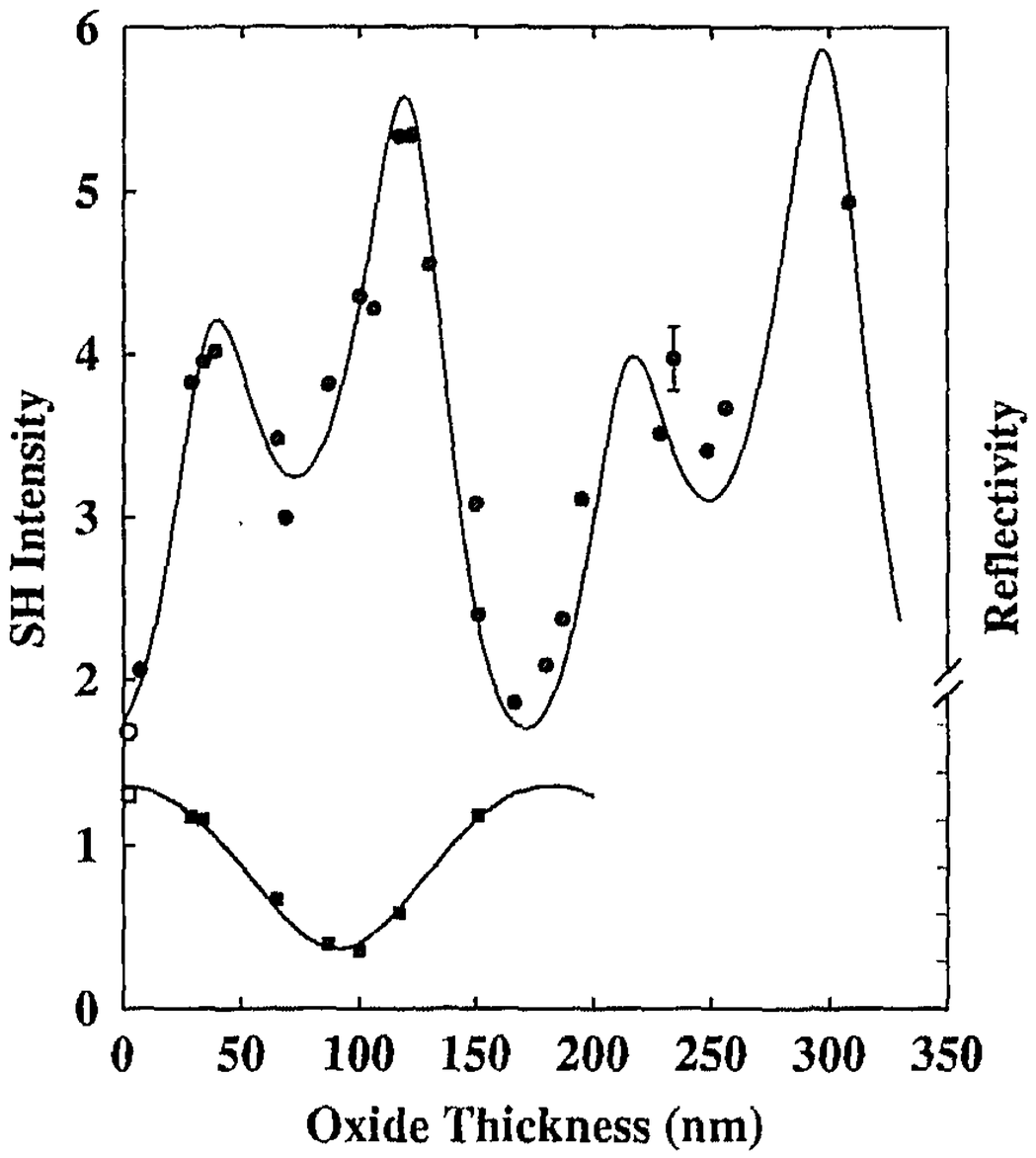

Fig. 2. Amplitude of $I_{s,s}$ (circles, left-hand vertical axis) and linear reflection (squares, right-hand vertical axis) as a function of oxide thickness for a 4° angle of incidence. The open symbols represent measurements on a part of the sample that was etched clean and then oxidized again. The solid curves are models for both.

between thermal and native silicon oxides. This is beyond the scope of the present paper. The appearance of a maximum in the angular dependence can be understood in terms of the optical path length in the oxide film. For every oxide thickness there is an angle of incidence such that the multiple reflected fields interfere constructively at the Si–SiO_2 interface, leading to a higher field in the silicon and a higher SH response. For the generated SH field the argument is analogous.

This thickness dependence is more directly demonstrated in Fig. 2, where the amplitude of $I_{s,s}$ (circles) and linear reflection (squares) are plotted as a function of oxide thickness at an angle of incidence of 4°. These data clearly show oscillations that are well described by this multiple-reflection model (solid curves). The linear Fresnel factors L_ω and $L_{2\omega}$ show interference. Neglecting the difference in phase rotation on reflection from Si (which is negligible for the fundamental field at 532 nm but not for the SH field) and the dispersion in the oxide would yield a period for $L_{2\omega}$ that is exactly twice that of L_ω. Because of the phase rotation and the dispersion in the oxide, the curve for $L_{2\omega}$ shifts, and its period is no longer exactly half of that for L_ω. Thus the phase rotation leads to a shift of the interference peaks, and the dispersion leads to a gradual change of the peak heights. One can calculate that a maximum enhancement of $I_{s,s}$ at an angle of incidence of 4° is obtained for an oxide thickness of ~1200 nm. The open symbols at 2 nm are measured on a part of the sample that was etched clean and then put into air to acquire a thin native oxide again. These data are well described by the model curves for both the SHG and the linear reflectance. This means that the thermal oxide and the native oxide obtained after the thermal oxide is etched away actually have the same SHG response parameter χ. This suggests that these two interfaces are the same or that SHG is insensitive to the differences between them. In contrast to the example of Fig. 1 for a native oxide of unknown history, in this case the results at 2 nm are completely consistent with the thick oxides.

The changes in $I_{s,s}$ can thus be completely understood in terms of multiple reflections in the oxide film. The analysis is simplified by the fact that for this polarization the SHG can effectively be characterized by one parameter. The same applies to the *s*-polarized SHG for a *p*-polarized pump field, which also contains only anisotropic contributions. For the *p*-polarized SHG both isotropic and anisotropic contributions arise, and the number of contributing tensor elements increases. The SHG can then no longer be characterized by a single parameter χ. However, from Snell's law it follows that the propagation direction of light in a nonabsorbing film is independent of film thickness. The Fresnel formulas[20] show that for such a film and *s*-polarized (or *p*-polarized) light the amplitude of the reflected and the transmitted light depends on the film thickness, but the polarization is not changed. In our case the oxide film is nonabsorbing for both the fundamental and the SH frequency. This means that the orientation of $\mathbf{E}_\omega$ and $\mathbf{E}_{2\omega}$ with respect to the sample coordinate system is independent of oxide thickness, and the relative contributions to the SHG from the different tensor components will remain the same. So, if only multiple reflections play a role, with no other SHG source, then for $I_{p,p}$ the anisotropy scales with oxide thickness.

$I_{p,p}$ has been measured as a function of the angle of incidence upon the samples with 310 and 260-nm oxide thicknesses and on the reference sample. The results can be described by[3,17]

$$E_{p,p}(2\omega) = A + B\,\exp(i\Phi)\cos(3\psi)\,, \tag{4}$$

where A is the isotropic and B the anisotropic contribution, both containing several bulk and surface tensor elements that have different angle-of-incidence dependences, and Φ is the phase difference between A and B. In Figure 3 the ratio A/B is plotted for all three measurements. Note first that for all samples the ratio A/B is indeed not constant. For the reference sample (squares) the ratio $A/B = 1$ at an angle of incidence of 45°, in agreement with a number of experiments on Si(111) in air.[3–6] For 310 (circles) and 260 nm (triangles) the ratio A/B is the same as for the reference sample below 45°, above which they clearly deviate. These results suggest that there is an extra SHG source. This source could be trapped charges at the interface that give rise to a symmetry-breaking dc electric field.

In conclusion, we have shown that the effect of a thick oxide layer on the SHG from thermally oxidized Si(111) is dominated by linear optics, owing to multiple reflections in the oxide film. These multiple reflections can enhance the SHG significantly when compared with that for a native oxide sample and are not related to any SHG source in the oxide itself, as was suggested previously.[10,15] For the *s*-polarized SHG this leads to an overall scaling of the anisotropy, which contains only anisotropic contributions. For the *p*-polarized SHG, however, the form of the anisotropy is also changed, suggesting an extra SHG source. For native oxides of 2 nm one can of course

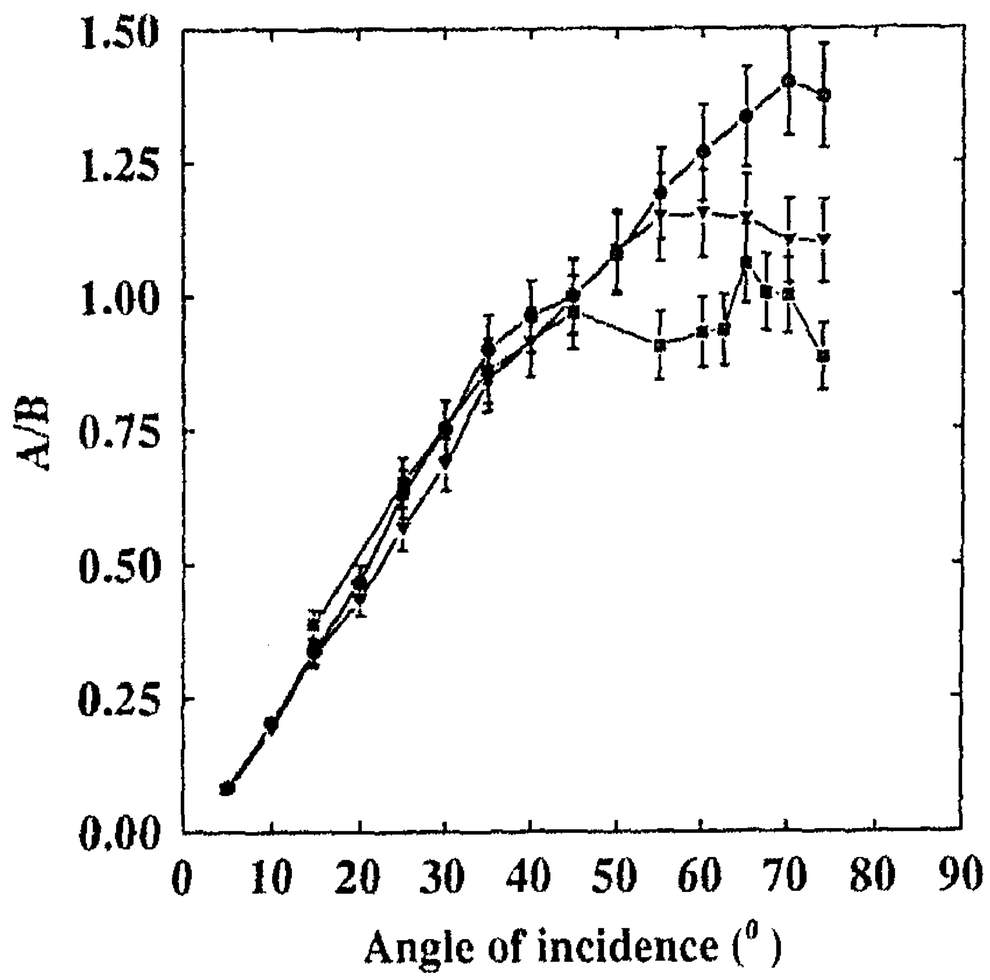

Fig. 3. Quotient A/B as a function of angle of incidence for oxide thicknesses of 310 (circles), 260 (triangles), and 2 nm (squares). A is the isotropic and B the anisotropic contribution to $I_{p,p}$. The solid curves are guides to the eye.

neglect the effects of multiple reflections. However, for these native oxides the SHG appears to depend on the sample preparation. These measurements show that one should be careful in analyzing the SHG from a buried interface and take into account the possibility of multiple reflections in the overlayer.

ACKNOWLEDGMENTS

We thank S. Bakker (University of Groningen) for preparation of the thick thermal oxide samples. O. A. Aktsipetrov thanks the Research Institute for Materials for their hospitality and for financial support. Part of this work was supported by the Stichting voor Fundamenteel Onderzoek der Materie, which is financially supported by the Nederlandse Organisatie voor Wetenschappelijk Onderzoek.

REFERENCES

1. Y. R. Shen, "Surface properties probed by second-harmonic and sum-frequency generation," Nature (London) **337,** 519–525 (1989).
2. G. L. Richmond, J. M. Robinson, and V. L. Shannon, "Second-harmonic generation studies of interfacial structure and dynamics," Prog. Surf. Sci. **28,** 1–70 (1988).
3. H. W. K. Tom, T. F. Heinz, and Y. R. Shen, "Second-harmonic reflection from silicon surfaces and its relation to structural symmetry," Phys. Rev. Lett. **51,** 1983–1986 (1983).
4. J. A. Litwin, J. E. Sipe, and H. M. van Driel, "Picosecond and nanosecond laser-induced second-harmonic generation from centrosymmetric semiconductors," Phys. Rev. B **31,** 5543–5546 (1985).
5. D. Guidotti, D. A. Driscoll, and H. J. Gerritsen, "Second harmonic generation in centrosymmetric semiconductors," Solid State Commun. **46,** 337–340 (1983).
6. C. W. van Hasselt, M. A. Verheijen, and Th. Rasing, "Vicinal Si(111) surfaces studied by optical second-harmonic generation: step-induced anisotropy and surface-bulk discrimination," Phys. Rev. B **42,** 9263–9266 (1990); "Optical second harmonic generation study of vicinal Si(111) surfaces," Surf. Sci. **251,** 467–471 (1991).
7. G. G. Malliaras, H. A. Wierenga, and Th. Rasing, "Study of the step structure of vicinal Si(110) surfaces using optical second harmonic generation," Surf. Sci. **287,** 703–707 (1993).
8. R. W. J. Hollering and M. Barmentlo, "Symmetry analysis of vicinal (111) surfaces by optical second-harmonic generation," Opt. Commun. **88,** 141–145 (1992).
9. W. Daum, H. J. Krause, U. Reichel, and H. Ibach, "Identification of strained silicon layers at Si–SiO_2 interfaces and clean Si surfaces by nonlinear optical spectroscopy," Phys. Rev. Lett. **71,** 1234–1237 (1993).
10. S. V. Govorkov, N. I. Koroteev, G. I. Petrov, I. L. Shumay, and V. V. Yakovlev, "Laser nonlinear-optical probing of silicon/SiO_2 interfaces: surface stress formation and relaxation," Appl. Phys. A **50,** 439–443 (1990).
11. O. A. Aktsipetrov and E. D. Mishina, "Nonlinear optical electroreflection in germanium and silicon," Sov. Phys. Dokl. **29,** 37–39 (1984).
12. C. H. Bjorkman, C. E. Shearon, Y. Ma, T. Yasuda, G. Lucovsky, U. Emmerichs, C. Meyer, K. Leo, and H. Kurz, "Second-harmonic generation in Si–SiO_2 heterostructures formed by chemical, thermal, and plasma-assisted oxidation and deposition processes," J. Vac. Sci. Technol. A **11,** 964–970 (1993); "Influence of surface roughness on the electrical properties of Si–SiO_2 interfaces and on second-harmonic generation at these interfaces," J. Vac. Sci. Technol. B **11,** 1521–1527 (1993).
13. G. Lüpke, D. J. Bottomley, and H. M. van Driel, "SiO_2/Si interfacial structure on vicinal Si(100) studied with second-harmonic generation," Phys. Rev. B **47,** 10389–10394 (1993).
14. O. A. Aktsipetrov, I. V. Kravetskii, L. L. Kulyuk, E. E. Strumban, and D. A. Shutov, "Second-harmonic generation upon reflection from a SiO_2/Si interface: the role of the crystalline transition layer," Sov. Tech. Lett. **15,** 719–720 (1989).
15. U. Emmerichs, C. Meyer, K. Leo, H. Kurz, C. H. Bjorkman, C. E. Shearon, Y. Ma, T. Yasuda, and G. Lucovsky, "Chemically modified second harmonic generation at surfaces on vicinal Si(111) wafers," Mat. Res. Sci. Symp. Proc. **281,** 815–820 (1992).
16. O. A. Aktsipetrov, I. M. Baranova, and Yu. A. Il'inskii, "Surface contribution to the generation of reflected second-harmonic light for centrosymmetric semiconductors," Sov. Phys. JETP **64,** 167–173 (1986).
17. J. E. Sipe, D. J. Moss, and H. M. van Driel, "Phenomenological theory of optical second- and third-harmonic generation from cubic centrosymmetric crystals," Phys. Rev. B **35,** 1129–1141 (1987).
18. R. W. J. Hollering, "Angular dependence of optical second-harmonic generation at a Ge(111) surface," J. Opt. Soc. Am. B **8,** 374–377 (1991).
19. Y. R. Shen, *The Principles of Nonlinear Optics* (Wiley, New York, 1984).
20. M. Born and E. Wolf, *Principles of Optics* (Pergamon, Oxford, 1980).
21. D. S. Bethune, "Optical harmonic generation and mixing in multilayer media: extension of optical transfer matrix approach to include anisotropic materials," J. Opt. Soc. Am. B **8,** 367–373 (1991).
22. M. S. Yeganeh, J. Qi, J. P. Culver, A. G. Yodh, and M. C. Tamargo, "Interference in reflected second-harmonic generation from thin nonlinear films," Phys. Rev. B **46,** 1603–1610 (1992).
23. D. E. Aspnes and A. A. Studna, "Dielectric functions and optical parameters of Si, Ge, GaP, GaAs, GaSb, InP, InAs, and InSb from 1.5 to 6.0 eV," Phys. Rev. B **27,** 985–1009 (1983).
24. E. D. Palik, ed., *Handbook of Optical Constants of Solids* (Academic, New York, 1985).